ELSEVIER

Journal of Nuclear Materials 258–263 (1998) 1178–1182

journal of nuclear materials

Microstructure assessment of the low activation ferritic/martensitic steel F82H

R. Schäublin *, P. Spätig, M. Victoria

EURATOM-Association-Swiss Confederation, CRPP-EPFL, 5232 Villigen PSI, Switzerland

Abstract

The microstructure of the low activation F82H ferritic/martensitic steel has been investigated in the cases of the heat treated, irradiated and deformed material. The irradiation has been achieved with 590 MeV protons in the Proton IRradiation EXperiment (PIREX) facility to a dose of 0.5 dpa at a temperature of 523 K. The unirradiated material was deformed in tension to failure at room temperature. The dislocations character as well as the dislocation density are determined. The carbide chemical composition and the size distribution of the carbides are assessed.

1. Introduction

The ferritic/martensitic steels are candidates for the future fusion reactor structural components where doses above 100 dpa are expected. Even though these steels have proved to be a good alternative to austenitic steels, with respect to swelling resistance, there are a number of problems related to the changes in mechanical properties and to the activation under irradiation. In response to the latter point the chemical composition of the ferritic/martensitic steel F82H has been designed to obtain a reduced long term radioactivity. Owing to the complexity of the microstructure the mechanical properties are expected to depend on the chemical composition, the pre-austenite grain (PAG) sizes, the martensitic lath sizes, the carbide size distribution and composition, and the dislocation microstructure.

Irradiation is known to drive the microstructure to both the formation of He bubbles [1,2], and to a change in the dislocation configuration [2–5]. The He production rate for fusion 14 MeV neutron is 13 appm/dpa [6] and about 130 appm/dpa for 590 MeV protons, but the effect of the He on the mechanical properties is believed to be small [7,8]. H production is about 800 appm/dpa for 590 MeV protons [9] but rapidly escapes the material. The relative resistance of ferritic/martensitic steels to swelling which increases at a rate of about 1% for 100 dpa [10] as compared to the 1% for 10 dpa for austenitic steels has to be explained by the fact that the irradiation induced vacancies are impeded to form voids. Several models were proposed in that sense on the basis of (1) a trapping mechanism of the interstitial and vacancies to impurities and alloying elements [10] that increases recombination, (2) the trapping of both type of point defects on dislocations with a Burgers vector of $a/2\ \langle 1\ 1\ 1\rangle$, and (3) the point defect bias to dislocations being inherently lower in the bcc than in the fcc structure, the effect of the presence of dislocations with a Burgers vector equal to $a\ \langle 1\ 0\ 0\rangle$ which trapping of interstitials leads to vacancy accumulation [4] is reduced. In the ferritic/martensitic steels the dislocation structure after irradiation develops dislocations with both $a/2\ \langle 1\ 1\ 1\rangle$ and $a\ \langle 1\ 0\ 0\rangle$ Burgers vectors, the latter being predominant when the Cr content is below the one of Fe–6Cr [2]. The $a/2\ \langle 1\ 1\ 1\rangle$ is the most common Burgers vector in the bcc structure [10] whilst irradiation induced dislocations with the $a\ \langle 1\ 0\ 0\rangle$ Burgers vector arises from the growth of $a\ \langle 1\ 0\ 0\rangle$ interstitial loops [5].

A TEM study of the F82H microstructure is presented here. The mechanical properties and the chemical behavior of the F82H steel are presented elsewhere [11,12].

* Corresponding author. Tel.: +41-56 310 4082; fax: +41-56 310 4529; e-mail: schaublin@psi.ch.

0022-3115/98/$19.00
PII: S0022-3115(98)00182-2

2. Experimental

The ferritic/martensitic steel denominated F82H [13] have a composition of about 7.65 wt% Cr, 2 wt% W, and Mo, Mn, V, Ta, Ti, Si and C below 1 wt% in sum total, and Fe for the balance. The samples were submitted to the heat treatment (0.5 h at 1313 K for normalization and 2 h at 1013 K for tempering) that allows to obtain a fully martensitic structure.

The irradiation has been performed in the PIREX facility located in the Paul Scherrer Institut of Villigen, Switzerland, with protons of 590 MeV at a temperature of 523 K to a dose of 0.5 dpa. The unirradiated sample was deformed in tension until failure on a Schenck RMC100 machine at 300 K. The TEM discs of the deformed specimen were taken from the uniform deformation region.

The 100 μm thick 3 mm TEM discs were prepared electrochemically (10 vol% perchloric acid, methanol) at 0°C and 30 V. Carbide size distribution measurement were achieved on extractions on carbon foils supported on Al grids. TEM observations and EDS measurements were conducted in the Centre Interdépartemental de Microscopie Electronique (CIME), EPFL, on a Philips LaB_6 CM20 operated at 200 kV. The high resolution observations were performed on a Philips FEG CM300 operated at 300 kV. The magnetism of the ferritic/martensitic steels requires particular attention to both objective astigmatism and beam tilt. The latter is corrected by recalling in diffraction mode the correct transmitted beam position recorded at the beginning of the session.

The carbide size distribution was investigated on both transmission and extracted samples. The dislocation Burgers vector were analyzed using the **g·b** analysis with a double-tilt side entry sample holder using the following procedure that provides four ⟨0 1 1⟩-type **g**'s and two ⟨2 0 0⟩-type **g**'s. The sample was tilted in order to reach a ⟨1 1 1⟩ zone axis, e.g. [1 1 1], that shows three different **g**'s of the ⟨0 1 1⟩ type, namely [1 0 $\bar{1}$], [0 $\bar{1}$ 1] and [1 $\bar{1}$ 0]. From this zone axis one **g** is selected, e.g. [1 $\bar{1}$ 0], and kept in order to reach by a 54.74° tilt of the specimen a ⟨0 0 2⟩ zone axis, e.g. [0 0 2]. The diffraction pattern is then composed of the [1 $\bar{1}$ 0] **g**, its normal **g** = [1 1 0] and two ⟨2 0 0⟩-type **g**, namely [2 0 0] and [0 2 0]. The three known Burgers vector in bcc structure, i.e. $1/2a_0$ ⟨1 1 1⟩, a_0 ⟨1 0 0⟩ and a_0 ⟨1 1 0⟩ [14], were accounted for in the analyses. The dislocation density was measured by counting the number of intersections of the dislocation with the free surfaces and by using the correction factors necessary to account for both the lack of visibility of a part of the dislocation population when using a given **g** diffraction vector and the unknown thickness [15].

3. Results and discussion

The micrographs of the general microstructure of the F82H heat treated (Fig. 1(a)), deformed (Fig. 1(b)) and irradiated (Fig. 1(c)) show common features characterized by both PAG boundaries and martensite laths. The martensite laths are about 1 μm wide and can reach more than 5 μm in length as it is clearly visible on Fig. 1(a). The lattice parameter of the heat treated F82H was measured with the diffraction patterns and the value averaged on three patterns obtained on different TEM sessions is 3.09 Å.

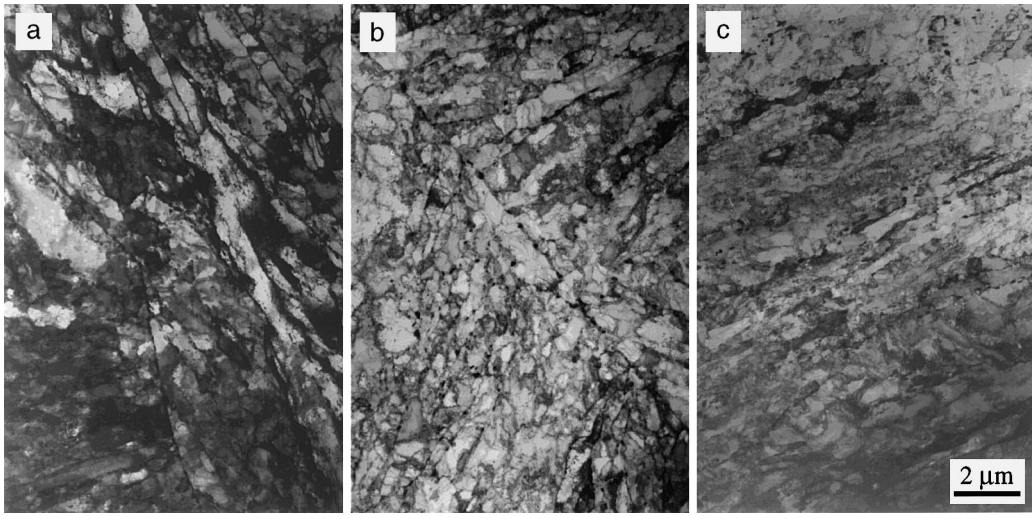

Fig. 1. TEM micrographs showing the basic microstructural features of the F82H material: (a) heat treated, (b) deformed, and (c) irradiated at 0.5 dpa at 523 K.

The dislocations in the heat treated F82H appear to be entangled (Fig. 2), with the common to bcc structure burgers vector equal to $1/2a_0\ \langle 1\ 1\ 1\rangle$. Neither $a_0\ \langle 1\ 0\ 0\rangle$ nor $a_0\ \langle 1\ 1\ 0\rangle$ Burgers vector were evidenced. The few straight segments appear to have a screw character. The deformed F82H contains dislocations that have a burgers vector equal to $1/2a_0\ \langle 1\ 1\ 1\rangle$ (Fig. 3). Fig. 3(b) shows clearly that the dislocations are straighter than in the heat treated specimen. The character of the dislocation is screw. Dislocations in the irradiated F82H have

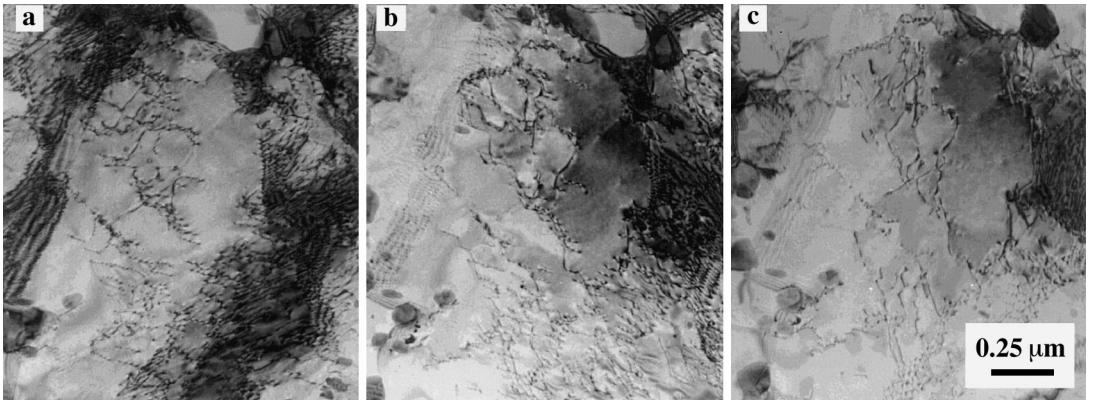

Fig. 2. **g**·**b** analysis of the heat treated F82H material. TEM micrographs taken with: (a) $\mathbf{g}=[\bar{1}\ 1\ 0]$, (b) $\mathbf{g}=[0\ 1\ \bar{1}]$, and (c) $\mathbf{g}=[1\ 0\ \bar{1}]$.

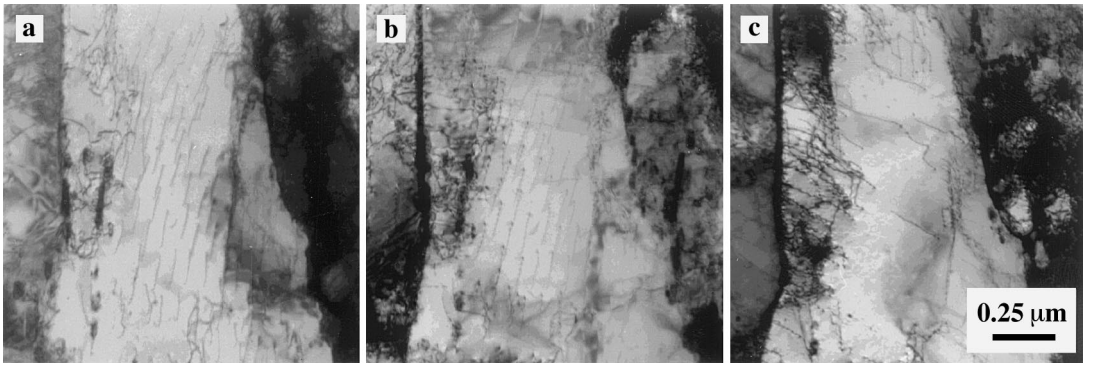

Fig. 3. **g**·**b** analysis of the deformed F82H material. TEM micrographs taken with: (a) $\mathbf{g}=[\bar{1}\ \bar{1}\ 0]$, (b) $\mathbf{g}=[2\ 0\ 0]$, and (c) $\mathbf{g}=[1\ 0\ \bar{1}]$.

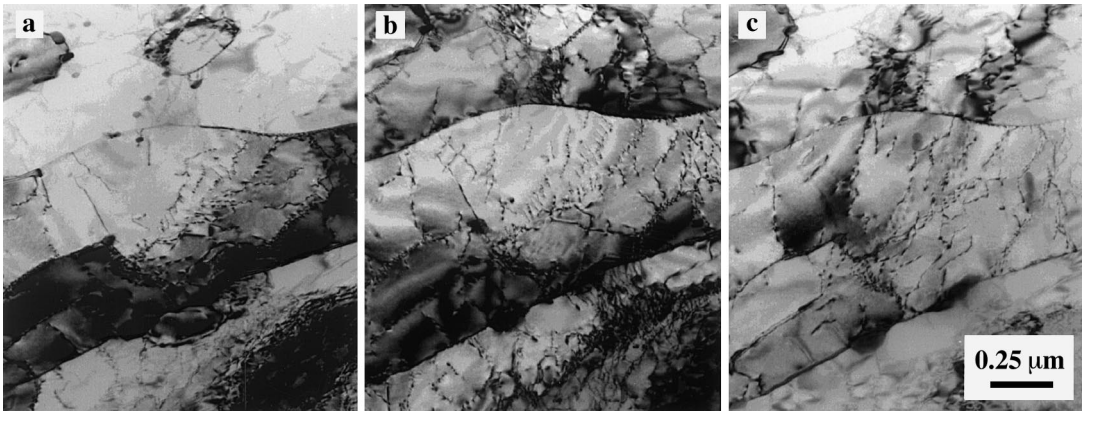

Fig. 4. **g**·**b** analysis of the F82H material irradiated at 0.5 dpa at 523 K. TEM micrographs taken with: (a) $\mathbf{g}=[\bar{1}\ 0\ 1]$, (b) $\mathbf{g}=[\bar{1}\ 1\ 0]$, and (c) $\mathbf{g}=[0\ 1\ \bar{1}]$.

a burgers vector equal to $1/2a_0\ \langle 1\ 1\ 1\rangle$ (Fig. 4), with a dominating screw character.

The dislocation density in the heat treated, in the deformed and in the irradiated material is, respectively, 0.86×10^{10}, 1.0×10^{10} and 0.9×10^{10} dislocation/cm^2, with a statistical error of ±20%. Within the error margin there is no difference in the dislocation density between the three different specimens. These values are in agreement with those found in the literature [2,3].

Carbides are present on the PAG boundaries, the lath boundaries and in the bulk of the martensite lathes. The carbides have an average composition of 60.6 at.% Cr, 28.8 at.% Fe, 6.3 at.% W, and traces in variable amounts of Ta, V and Ti. The carbides are close in composition to the common $M_{23}C_6$, that has an orthorhombic structure [16]. A CBED pattern analysis confirmed that the carbides have an orthorhombic structure. Furthermore it appears that bulk carbides are generally coherent with the matrix. Fig. 5 shows a HREM micrograph of the interface region between a bulk carbide of about 30 nm in diameter and the matrix. The power spectra shows that the $\langle 0\ 1\ 1\rangle$ direction of the matrix is parallel to the $\langle 1\ 1\ 1\rangle$ direction of the carbide. The white line shows that there is a common $\{0\ 1\ 1\}$ plane between the matrix and the carbide. The $\{0\ 1\ 1\}$ plane images shows that there is no mismatch dislocation in this direction between the two structures.

The carbide sizes range from 10 to 500 nm in all studied materials, for an average size of 43, 47 and 49 nm for, respectively, the heat treated material (Fig. 6(a)), the deformed (Fig. 6(b)) and the irradiated material (Fig. 6(c)). Hence the three studied material do not show significant changes within the statistical error in mean size or size ranges relatively to the heat treated material. The chemical composition of the carbides in the deformed and the irradiated material do no deviate from the ones in the heat treated sample. It should be noted that the peak in the small sizes of the carbide distribution is due to the relative large number of carbides with sizes below 10 nm. It does not reflect a bimodal size distribution.

The heat treated, deformed and the F82H material irradiated at 0.5 dpa at 523 K show similar dislocation configurations, with straighter screw dislocations for the deformed material. The carbide size distribution, mean size, composition and structure are equivalent within the three different materials. The similarity of the microstructure characteristics between the heat treated and the deformed specimens can be explained by the fact that the microstructure in the heat treated specimen contains a high residual internal stress induced by the heat treatment, even though the tempering temperature (1073 K) is chosen for a minimum of heat treatment induced hardening. It leads to a microstructure similar to the one derived from a deformation.

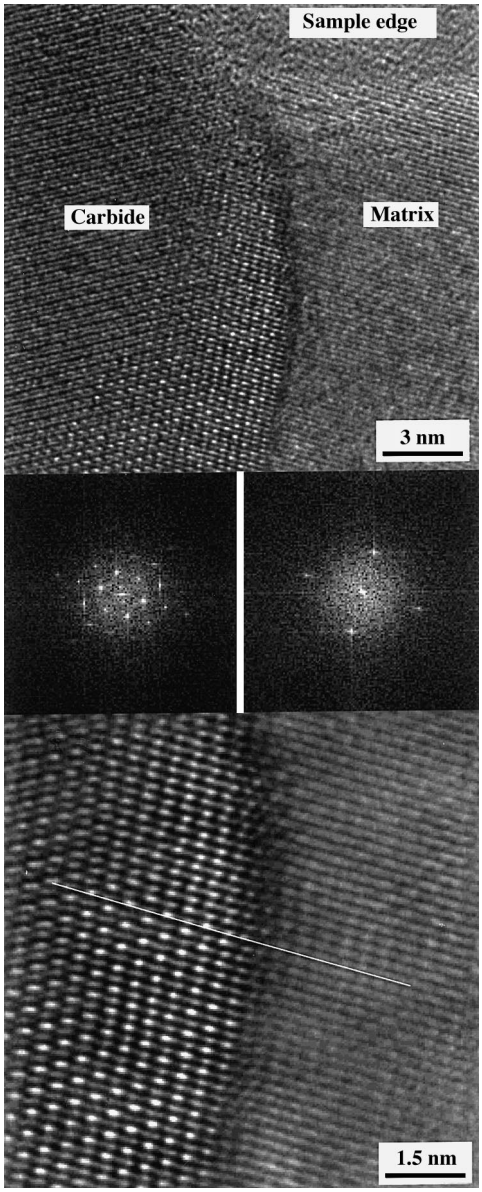

Fig. 5. Coherency between the carbides and the matrix in F82H heat treated shown in a high resolution TEM micrograph (top image). Power spectra of the carbide (middle left) and of the matrix (middle right). The white line on the Fourier filtered enlarged image (bottom) indicates a common crystallographic plane.

No irradiation defects such as dislocation loops or He bubbles were observed in the 0.5 dpa irradiated specimen, for the latter probably because of the relatively low irradiation temperature. Moreover, a close observation by weak beam TEM $\mathbf{g}(6\mathbf{g})$ with $\mathbf{g} = \langle 0\ 1\ 1\rangle$ showed that there is no irradiation induced precipitates, such as the chromium rich α' phase precipitates, as

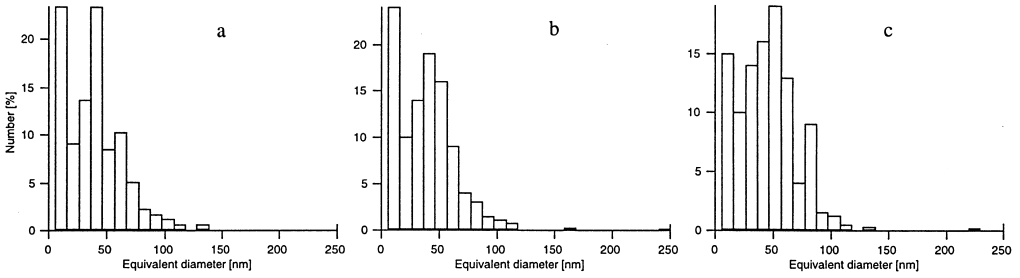

Fig. 6. Carbide size distribution of F82H for the (a) heat treated material, (b) deformed material and (c) the material irradiated at 0.5 dpa at 523 K.

suggested in [2]. The lack of visible differences in the microstructure between the unirradiated and the irradiated specimen is certainly related to the relatively low dose explored so far in this study. However, chemical segregation behavior differences were observed between the unirradiated and the irradiated specimens [12].

4. Conclusion

The dislocation structure of the F82H ferritic/martensitic steel consists of $1/2a_0$ $\langle 1\ 1\ 1 \rangle$ Burgers vector dislocations. It appears that there is a strong tendency to screw character orientation in the unirradiated and specimens irradiated to 0.5 dpa, which suggests a Peierls mechanism. No differences in either the carbide microstructure, composition or the size distribution were found between unirradiated and irradiated specimens.

Acknowledgements

Dr David Gelles is acknowledged for his advices on the observation in TEM of magnetic specimens.

References

[1] E.A. Little, D.A. Stow, J. Nucl. Mater. 87 (1979) 25.
[2] D. S. Gelles, J. Nucl. Mater. 108/109 (1982) 515.
[3] Y. Katoh, A. Kohyama, D.S. Gelles, J. Nucl. Mater. 225 (1995) 154.
[4] R. Bullough, M.H. Wood, E.A. Little, Effects of Radiation on Materials: 10th conference, ASTM STP 725, D. Kramer, H.R. Brager, J.S. Perrin Eds., ASTM (1981) 593.
[5] E.A. Little, R. Bullough, M.H. Wood, Proc. Roy. Soc. London A372 (1980) 565.
[6] M.S. Wechsler, D.R. Davidson, L.R. Greenwood, W.F. Sommer, Effects of Radiation on Materials: 12th conference, ASTM STP 870, F.A. Garner, J.S. Perrin Eds., ASTM (1985) 1189.
[7] K.K. Bae, K. Ehrlich, A. Möslang, J. Nucl. Mater. 191–194 (1992) 905.
[8] K. Shiba, M. Suzuki, A. Hishinuma, J.E. Pawel, Effects of Radiation on Materials: Tenth conference, ASTM STP 1270, D.S. Gelles, R.K. Nanstad, A.S. Kumar, E.A. Little Eds., ASTM (1996) 753.
[9] S.L. Green, J. Nucl. Mater. 126 (1984) 30.
[10] E.A. Little, J. Nucl. Mater. 87 (1995) 11.
[11] P. Spätig, R. Schäublin, S. Gyger, M. Victoria, these Proceedings.
[12] R. Schäublin, P. Spätig, M. Victoria, these Proceedings.
[13] M. Tamura, H. Hayakawa, M. Tanimura, A. Hishinuma, T. Kondo, J. Nucl. Mater. 141–143 (1986) 1067.
[14] R.W.K. Honeycombe, The plastic deformation of metals, W. Clowes & Sons, London (1975) 111.
[15] P.B. Hirsch, A. Howie, R.B. Nicholson, D.W. Pashley, M.J. Whelan, Electron Microscopy of Thin Crystals (Butterworths, London 1969), 422.
[16] J.H. Woodhead, A.G. Quarrell, J. Iron Steel Inst. (1965) 605.